# Two mechanisms by which fluorescent oxonols indicate membrane potential in human red blood cells

Promod R. Pratap, Terri S. Novak, and Jeffrey C. Freedman
Department of Physiology, State University of New York Health Science Center, Syracuse, New York 13210

ABSTRACT Optical potentiometric indicators have been used to monitor the transmembrane electrical potential ($E_m$) of many cells and organelles. A better understanding of the mechanisms of dye response is needed for the design of dyes with improved responses and for unambiguous interpretation of experimental results. This paper describes the responses to $\Delta E_m$ of 20 impermeant oxonols in human red blood cells. Most of the oxonols interacted with valinomycin, but not with gramicidin. The fluorescence of 15 oxonols decreased with hyperpolarization, consistent with an "on-off" mechanism, whereas five oxonols unexpectedly showed potential-dependent increases in fluorescence at <2 μM [dye]. Binding curves were determined for two dyes (WW781, negative response and RGA451, positive response) at 1 mM $[K]_o$ (membrane hyperpolarized with gramicidin) and at 90 mM $[K]_o$ ($\Delta E_m = 0$ with gramicidin). Both dyes showed potential-dependent decreases in binding. Changes in the fluorescence of cell suspensions correlated with changes in $[dye]_{bound}$ for WW781, in accordance with the "on-off" mechanism, but not for RGA451. Large positive fluorescence changes (>30%) dependent on $E_m$ were observed between 0.1 and 1.0 μM RGA451. A model is suggested in which RGA451 moves between two states of different quantum efficiencies within the membrane.

## INTRODUCTION

Dyes that respond to a change in membrane potential, $E_m$, with a change in some optical property were designed originally to study electrical activity in neural systems (see London et al., 1988, for review), and have since proved useful in other excitable tissues, and also in suspensions of nonexcitable cells, including red blood cells (see Waggoner, 1979; Freedman and Laris, 1981, 1988 for reviews). Fluorescent potentiometric indicators are frequently used to measure changes in membrane potentials ($\Delta E_m$) of small cells and organelles, or in other situations where microelectrodes cannot be used.

Potentiometric dye signals may either be "fast" (microseconds to milliseconds), or "slow" (seconds), reflecting at least two classes of mechanisms. The signal depends on the particular dye, system, and protocol used to measure $\Delta E_m$. For example, the fluorescent cyanine, diS-$C_3$(5), responds slowly in red blood cells when equilibrium or diffusion potentials are measured (Hoffman and Laris, 1974; Freedman and Hoffman, 1979*a*, *b*); the same dye responds rapidly in planar lipid bilayers subjected to voltage pulses of millisecond duration (Waggoner et al., 1977).

Understanding the mechanisms by which dyes respond is important for interpreting experimental results and for designing new indicators with improved ratios of signal-to-noise and with reduced toxicity to cells. In addition, an understanding of dye-membrane interactions could enhance insight into the dielectric properties of the membrane and into electric potential profiles across the membrane (Apell and Bersch, 1987).

The mechanism of action of the slow cyanine dyes has been studied in suspensions of red blood cells (Sims et al., 1974; Hladky and Rink, 1976; Tsien and Hladky, 1978; Freedman and Hoffman, 1979*b*; Guillet and Kimmich, 1981), in renal brush-border vesicles (Cabrini and Verkman, 1986*a*, *b*), and in phospholipid vesicles (Guillet and Kimmich, 1981). In red cells, the action of diS-$C_3$(5) has been described by an eight-parameter model in terms of potential-dependent bulk redistribution of dye between the inside and outside of cells, with shifts between dye monomers and dimers (Sims et al., 1974; Hladky and Rink, 1976; Tsien and Hladky, 1978). Support for monomer-dimer shifts comes from spectral studies (Hladky and Rink, 1976; Freedman and Hoffman, 1979*b*). Other cyanines, such as diI-$C_3$(5) and diO-$C_3$(5), exhibit no detectable monomer-dimer shift (Freedman and Hoffman, 1979*b*; Guillet and Kimmich, 1981).

In contrast to the cyanines, the response of a permanent oxonol dye, OX-V, in phospholipid vesicles is biphasic, with a fast phase due to changes in dye binding to the membrane, and a slow phase due to translocation of dye across the membrane (Bashford et al., 1979). The voltage

Address correspondence to Dr. Freedman


0006-3495/90/04/835/15 $2.00

dependence of the partition coefficient of a related oxonol, OX-VI, between the membrane and the aqueous phase has been described in terms of a three-capacitor model, and this dye has been used to measure electrogenic potentials generated by the Na/K pump reconstituted in phospholipid vesicles (Apell and Bersch, 1987).

Interpretation of signals with permeant dyes is compromised by potentials that may exist across the membranes of internal organelles. Moreover, the slow response of permeant dyes precludes study of changes in $E_m$ that occur with half-times of milliseconds or less. Also, the response of the slow cyanine dye diS-$C_3$(5) in red cells is linear with voltage from $\sim+50$ to $-40$ mV (Hladky and Rink, 1976; Freedman and Hoffman, 1979*b*; Bifano et al. 1984), a range that is insufficient to characterize the voltage dependence of Cl conductance. Some of these problems may be circumvented by use of impermeant fast dyes, whose signals are smaller yet linear over a larger range of voltages than the permeant cyanines (Freedman and Novak, 1983, 1989). However, because fast dyes are membrane-bound, they may interfere with membrane transport systems. For example, the response of the fast oxonol dye WW781, is linear for a range of at least 100 mV in red cells, but this dye stimulates Cl conductance that is sensitive to DIDS (4,4′-diisothiocyanatostilbene-2,2′-disulfonic acid), but not DIDS-insensitive Cl conductance (Freedman and Novak, 1983, 1989; Freedman et al., 1988). A fast dye with minimal toxicity is needed for the study of conductive pathways in the red blood cell such as Cl conductance, Ca-activated K conductance, and electrogenic modes of the Na/K pump.

Fast dyes themselves operate by several different mechanisms. In squid giant axons and model membranes, merocyanine-540 reports $\Delta E_m$ by reorientation within the membrane and by monomer-dimer shifts (Ross et al., 1974; Dragsten and Webb, 1978; Wolf and Waggoner, 1986), but no potentiometric signals with this dye were detected in red blood cells. Other fast dyes were designed to optimize electrochromic shifts and exhibited this mechanism in hemispherical bilayers (Loew and Simpson, 1981; Fluhler et al., 1985), but were subsequently found to act by other mechanisms when tested in the squid giant axon (Loew et al., 1985).

The fast oxonol WW781 and its analogues are presumed to be impermeant because of their fast response times and because a fixed negative charge anchors the dye to the outside of the membrane. In hemispherical bilayers, impermeant oxonols report $\Delta E_m$ by dye redistribution between the external aqueous buffer and the membrane, an "on-off" mechanism (Waggoner and Grinvald, 1977; George et al., 1988*a*, *b*; Nyirjesy et al., 1988). Over 350 other fast dyes have been screened for their usefulness in the squid giant axon (Gupta et al., 1981).

This paper describes results of a survey of 20 impermeant oxonols; the goal was to find a rapidly responding dye with minimal toxic effects on red blood cells. The oxonols chosen are part of a larger set surveyed by George et al. (1988*a*, *b*) and Nyirjesy et al. (1988) in hemispherical bilayers. The results showed unexpectedly that certain impermeant oxonols respond by a new mechanism. Consequently, two oxonols were selected to study the correlation between their fluorescence responses and membrane binding.

## MATERIALS AND METHODS

### Preparation of cells and ghosts

Fresh blood from healthy human donors was drawn by venipuncture into heparinized vacutainers, and centrifuged at 13,800 *g* for 3 min at 4°C. The plasma and buffy coat were aspirated, and the cells were washed three or four times by centrifugation, each time resuspending in ~5 vol of chilled washing medium. In experiments with valinomycin the washing medium contained 1 mM KCl, 149 mM NaCl, and 5 mM Hepes (*N*-2-hydroxyethylpiperazine-*N*′-2-ethane-sulfonic acid; Sigma Chemical Co., St. Louis, MO), pH 7.4 at 25°C. In experiments with gramicidin D, NaCl was replaced in equimolar amounts either by choline chloride or *N*-methyl-D-glucamine (Sigma Chemical Co.). The packed cells were diluted with washing medium to 50% hematocrit (HCT), and kept on ice for use on the same day.

Leaky white ghosts were prepared by the method of Dodge et al. (1963), and were also diluted to 50% HCT in the cell washing medium. A cell counter (model ZBI; Coulter Corporation, Hialeah, FL) was used to ensure that the number of ghosts per milliliter in the cuvette was equivalent to that of cells.

### Dye survey

The 20 oxonols surveyed were gifts from Dr. A. S. Waggoner, Department of Biological Sciences, Carnegie Mellon University, Pittsburgh, PA. Stock solutions of dyes (0.1, 1 and 10 mg/ml) were prepared in absolute ethanol, as were valinomycin (2.78 mg/ml, 2.5 mM, 1,111 g/mol; Calbiochem-Behring Corp., La Jolla, CA) and gramicidin D (0.33 mg/ml; Sigma Chemical Co.). The dye responses (%$\Delta F$) to changes in $E_m$ were measured at systematically varied [dye] and HCT at 23°C as described elsewhere (Freedman and Novak, 1989). The response, $R$, of the dye to changes in $E_m$ is defined as

$$R = 100 \cdot (F^{+1} - F^{-1})/F^{-1}, \quad (1)$$

where $F^{-1}$ and $F^{+1}$ are the fluorescence of the cell suspension before and after adding ionophore.

### Dye fluorescence and absorption

Dye fluorescence was measured with a photon counting spectrofluorometer (model 8000S; SLM-Aminco, Urbana, IL) equipped with a 450 W Xenon arc lamp, double grating excitation monochromator set at the maximum of the excitation spectrum (e.g., 615 nm for WW781 and RGA451) with 16-nm bandpass, and a model R928P photomultiplier tube (Hamamatsu Corp., Middlesex, NJ). Uncorrected excitation and emission spectra were measured at 1 nm/s with both the excitation and emission monochromators in place. A polarizer oriented at 0° was placed

in the path of the emission beam to minimize the effects of the Woods anomaly. For kinetic measurements, the emission monochromator was replaced with a cutoff filter (e.g., RG645 for WW781 and RGA451; Schott Optical Glass, Duryea, PA) in series with a frosted quartz screen, and the polarizer was removed. Fluorescence was recorded on an X-Y recorder (model 7046B; Hewlett-Packard, San Diego, CA) and digitized with a tablet. Cuvettes (polyacrylic, No. 67.755; Sarstedt, Nümbrecht, FRG) contained 2.5 ml medium which was stirred with Teflon-coated magnetic bars, and which was thermostated at 23°C with a circulating water bath (Lauda K-2/RD; Brinkmann Instruments, Westbury, NY).

To survey parameters of dye binding (apparent dissociation constant, $K_d$, and number of binding sites per cell, $n$), each dye was added step-wise to a 1.2% HCT cell suspension until the fluorescence saturated. HCT was then varied at the [dye] giving maximum fluorescence. Curves of fluorescence vs. HCT were used to determine $K_d$, $n$, and the enhancement parameter $\epsilon_b$ (see Appendix). Binding of WW781 and RGA451 to intact red cells was also determined directly (see below).

Dye absorption spectra in buffer and in cell suspensions were determined on a double beam spectrophotometer (model DW-2 UV/VIS; SLM-Aminco, Urbana, IL). The light source was a 150-W tungsten projector lamp (FCS; Sylvania-GTE, Winchester, KY). Light was chopped between sample and reference and was passed through a ground glass plate and a beam scrambler to a photomultiplier tube (R562-HA; Hamamatsu Corp.). Spectra were recorded on the spectrophotometer X-Y recorder, and then digitized on a tablet (Kurta Series II).

## Measurements of dye binding

In addition to extracting apparent binding parameters indirectly from fitting the fluorescence data, dye binding curves were also measured directly for two dyes, WW781 and RGA451, before and after hyperpolarization by addition of gramicidin D. For both dyes, six cuvettes were prepared at each of five dye concentrations. Dye fluorescence in each cuvette was measured as described above. Dye absorbance in each cuvette was also measured (at 600 nm for WW781 and at 608 nm for RGA451) in a spectrophotometer (Cary 219) against a reference with medium. In each of the six cuvettes, a 0.2 ml portion of dye solution was replaced with an equivalent amount of the 50% HCT suspension, and the fluorescence of this 4% HCT suspension was recorded. Three of the cuvettes at each [dye] were centrifuged at 1720 × $g$ for 5 min, and the absorbance of each supernatant was recorded. To each of the three remaining cuvettes, 2.4 μl of 0.33 mg/ml gramicidin D (in ethanol) was added, and the fluorescence of each suspension was recorded. The cuvettes were then centrifuged and the absorbance of each supernatant was measured. To normalize the results, the HCT of the 50% stock suspension was measured, and a portion was hemolyzed and diluted with Drabkin's reagent. Hemoglobin (g Hb/ml) was then measured at 540 nm against cyanmethemoglobin standards (Boehringer Mannheim, Inc., Indianapolis, IN).

## Analysis of dye binding

The initial absorbance as a function of [dye], averaged for the six cuvettes, provided a standard curve for determination of the final [dye] in the supernatants. The difference between the amount of dye before addition of cells and after centrifuging each suspension is a measure of the amount of cell-associated dye, or $b$ (nmol/g $Hb$), given as follows:

$$b = (2.3\,d - 2.4\,s)/Hb, \qquad (2)$$

where $d$ and $s$ are the concentrations (μM) of dye before and after addition of cells, and $Hb$ is the hemoglobin (grams) in the cuvette. $Hb$ was determined from that measured in the stock suspension and the volume added to the cuvette. The factor 2.3 represents the volume of buffer in the cuvette before addition of cells; the factor 2.4 represents the volume of extracellular buffer. The total volume of the suspension was 2.5 ml, of which 0.1 ml was cells.

The apparent quantum efficiency (AQE) is defined as the ratio of fluorescence to [dye]. Because fluorescence is a nonlinear function of [dye], AQE varies with [dye]. A calibration curve of AQE vs. [dye], determined before addition of cells, was used to determine $AQE_s$, the apparent quantum efficiency of the supernatant free dye whose concentration, $s$ (μM), was measured by absorption after centrifuging the suspension. The apparent quantum efficiency of bound dye, $AQE_b$, was then calculated as follows:

$$AQE_b = (F - AQE_s s)/b, \qquad (3)$$

where $F$ is the measured fluorescence of the cell suspension, and $b$ is the amount of cell-associated dye.

Binding data are represented as plots of $[dye]_{bound}$ vs. $[dye]_{free}$ and as Scatchard plots ($[dye]_{bound}/[dye]_{free}$ vs. $[dye]_{bound}$). Bound dye as a function of total dye was first fit by Eq. A3 (see Appendix) with a nonlinear least-squares algorithm (Hamilton, 1964), yielding $K_d$ and $n$ for the single site model. When two or more populations of binding sites exist, the Scatchard plots can be expressed as the sum of two or more straight lines. Each slope equals $1/K_d$ for a particular site; each $x$ intercept gives the concentration of that site ($n$).

## Net efflux measurements

Net K and Cl effluxes from cells hyperpolarized with gramicidin in *N*-methyl-D-glucamine medium at 1 mM $[K]_o$ with varied [dye] were measured as described elsewhere (Freedman et al., 1988).

# RESULTS

This section first summarizes the results of the survey of the responses of twenty impermeant oxonols in intact red cells, with controls in leaky ghosts. From the survey, two dyes, WW781 and RGA451, were selected for further study. The spectral properties and responses to $\Delta E_m$ of these two dyes are compared, followed by a comparison of their voltage-induced changes in membrane binding.

## Dye survey

Table 1 summarizes the structures, absorption maxima, extinction coefficients, excitation and emission maxima and apparent binding parameters for the 20 oxonol dyes in the survey. The fluorescence of each dye was determined at varied [dye] and HCT; typical curves for WW781 at varied [dye] and HCT were given by Freedman and Novak (1983, their Fig. 2).

Table 1 also gives the wavelength ($\lambda_{abs}$) for maximal absorbance of each dye in ethanol, and the extinction coefficient ($\epsilon_{max}$) at this wavelength. These parameters were determined for each dye during the survey. For RGA451 and WW781, $\epsilon_{max}$ was also determined at the

**TABLE 1 Structure and optical properties of oxonol dyes**

| Dye | Structure* Y | $R_1$ | $R_2$ | $R_3$ | $R_4$ | $\lambda_{abs}$‡ | $\epsilon_{max}$‡ | $\lambda_{ex}$§ | $\lambda_{em}$§ | $K_d$ | $n$ | $\epsilon_b$ | $-CH_2-$‖ |
|---|---|---|---|---|---|---|---|---|---|---|---|---|---|
| | | | | | | *nm* | $(10^4/M)$ | *nm* | *nm* | μM | $\times 10^{-6}$ | | |
| WW781** | O | *A* | $C_1$ | $C_4$ | $C_4$ | 612 | 12.1 | 615 | 643 | 0.70 | 2.5 | 7 | 9 |
| WW802** | O | *A* | $C_1$ | $C_5$ | $C_5$ | 612 | 5.9 | 613 | 642 | 0.23 | 2.3 | 16 | 11 |
| RGA459‡‡ | O | *A* | $C_2$ | $C_4$ | $C_4$ | 612 | 9.6 | 614 | 640 | 0.72 | 1.7 | 11 | 10 |
| RGA461** | O | *A* | $C_2$ | $C_5$ | $C_5$ | 612 | 9.5 | 614 | 648 | 0.11 | 2.4 | 10 | 12 |
| RGA592** | O | *A* | $C_2$ | $C_6$ | $C_6$ | 612 | 12.4 | 614 | 648 | 0.04 | 3.7 | 28 | 14 |
| RGA570A‡‡ | O | *A* | $C_3$ | $C_5$ | H | 609 | 5.0 | 585 | 648 | 0.26 | 1.4 | 2.3 | 8 |
| RGA570‡‡ | O | *A* | $C_3$ | $C_5$ | $C_5$ | 612 | 11.8 | 614 | 648 | 0.14 | 1.1 | 27 | 13 |
| RGA485** | O | *A* | $C_5$ | $C_4$ | $C_4$ | 612 | 3.3 | 613 | 643 | 0.23 | 2.9 | 26 | 14 |
| RGA451‡‡ | O | *A* | $\phi$ | $C_3$ | $C_3$ | 618 | 11.3 | 615 | 652 | 0.33 | 1.1 | 15 | 10 |
| RGA512‡‡ | O | *A* | $CO_2Et$ | $C_3$ | $C_3$ | 625 | 25.4 | 615 | 658 | 0.30 | 0.7 | 57 | 8 |
| RGA514** | O | *A* | $CO_2Et$ | $C_5$ | $C_5$ | 625 | 14.9 | 614 | 661 | 0.10 | 1.0 | 16 | 12 |
| RGA497‡‡ | O | *A* | $CH_2CO_2Me$ | $C_4$ | $C_4$ | 615 | 15.4 | 608 | 642 | 0.83 | 1.1 | 6 | 10 |
| RGA500‡‡ | O | *A* | t-Butyl | $C_4$ | $C_4$ | 612 | 17.6 | 616 | 648 | 0.36 | 0.5 | 15 | 11 |
| RGA590** | O | *B* | $C_2$ | $C_5$ | $C_5$ | 612 | 6.8 | 613 | 645 | 0.33 | — | 12 | 12 |
| RGA466‡‡ | O | *C* | $C_1$ | $C_4$ | $C_4$ | 612 | 8.9 | 610 | 635 | 0.38 | 1.1 | 5 | 9 |
| RGA529‡‡ | O | *D* | $C_1$ | $C_4$ | $C_4$ | 614 | 5.8 | 615 | 645 | 0.26 | 1.1 | 151 | 12 |
| RGA33A** | S | *A* | $C_1$ | $C_4$ | $C_4$ | 622 | 6.7 | 622 | 652 | 0.03 | 1.3 | 42 | 9 |
| RGA339** | S | *A* | $C_1$ | $C_5$ | $C_5$ | 630 | 7.0 | 615 | 670 | 0.10 | 0.7 | 7 | 9 |
| RGA571** | S | *A* | $C_2$ | $C_4$ | $C_4$ | 633 | 6.8 | 614 | 668 | 0.19 | 1.4 | 21 | 10 |
| RGA567‡‡ | S | *A* | $CO_2Et$ | $C_2$ | $C_2$ | 649 | 21.5 | 615 | 682 | 0.44 | 0.8 | 9 | 6 |

*General structure of the dyes is

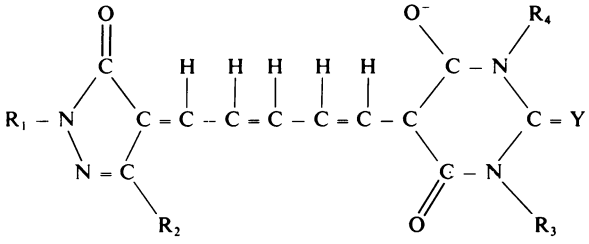

$R_1$, $R_2$, $R_3$, $R_4$ and Y are different for each dye. Key to groups represented in $R_1$ is: *A* = 4-sulfophenyl; *B* = 2-sulfophenyl; *C* = 2-chloro-5-sulfo-phenyl; *D* = 4-(7 sulfo-6-methyl-2 benzothiazoyl)-phenyl; $\phi$ = phenyl. C1 to C6 are alkyl chains.

‡$\lambda_{abs}$ = maximum of absorbance spectrum of dye in ethanol. $\epsilon_{max}$ = extinction coefficient of dye in ethanol at $\lambda_{abs}$.

§$\lambda_{ex}$, $\lambda_{em}$ = fluorescence excitation and emission maxima, determined from spectra of dye (2.7 μg/ml) in buffer.

‖Equivalent alkyl chain lengths; from Nyirjesy et al. (1988).

**The cells were suspended in medium containing 1 mM KCl, 149 mM NaCl, and 5 mM HEPES buffer, pH 7.4 at 25°C.

‡‡The NaCl in the suspension medium was replaced by choline chloride.

end of the series of binding experiments. In addition, the extinction coefficient of these two dyes was determined during the binding experiments. For WW781, $\epsilon_{max}$ for dye in ethanol was $1.21 \times 10^5$ $M^{-1}$ during the survey and $1.19 \times 10^5$ after the binding experiments. For RGA451, these values were $1.13 \times 10^5$ and $1.02 \times 10^5$ $M^{-1}$, respectively. In buffer, the average $\epsilon_{max}$ during the binding experiments was $0.90 \pm 0.11 \times 10^5$ $M^{-1}$ (SD, $n = 12$) for WW781 and $0.87 \pm 0.06 \times 10^5$ $M^{-1}$ (SD, $n = 11$) for RGA451. The $\epsilon_{max}$ in buffer of these two dyes at the end of the binding experiments were within two standard deviations of the average. Any large change in $\epsilon_{max}$ for either dye would have implied degradation of dye with storage.

The maximal responses, for the range of [dye] and HCT tested, for each dye upon hyperpolarization of the cells with gramicidin in choline medium at 1 mM external potassium concentration, or $[K]_o$, are shown in Fig. 1 *B* (*open bars*). As controls, the dye responses were also measured at 90 mM $[K]_o$ where the responses are expected to be small because K is near electrochemical equilibrium across the membrane (Fig. 1 *B*, *solid bars*). Additional controls were also performed with leaky white ghosts, which cannot support a membrane potential (Fig. 1 *A*). None of the dyes exhibited significant responses in white ghosts at 1 or 90 mM $[K]_o$, or in intact cells at 90 mM $[K]_o$.

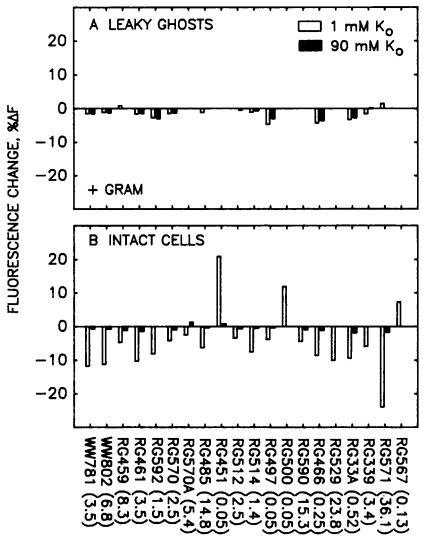


FIGURE 1 Survey of gramicidin-induced responses (%$\Delta F$) of 20 oxonols in intact human red blood cells (*B*), with controls in leaky ghosts (*A*). Hematocrit = 1.2% (except for RGA570A at 0.2% HCT). Extracellular medium contained $x$ mM KCl, (150 − $x$) mM choline Cl, where $x$ = 1 (*open bars*) or 90 (*solid bars*), and 5 mM Hepes, pH 7.4 at 25°C. Cells were hyperpolarized by adding gramicidin at 110 ng/ml of cell suspension. Lack of bar indicates 0 %$\Delta F$. Numbers in parentheses indicate $\mu$M [dye] for the maximal response obtained under the conditions tested.

As mentioned earlier, three dyes, RGA451, RGA500, and RGA567, unexpectedly showed increases instead of decreases in fluorescence upon hyperpolarization with gramicidin. Two other dyes, RGA459 and RGA497, gave positive responses in a low dye concentration range, but their negative responses at high [dye] were larger than their positive responses. Whereas the negative responses of the other 15 oxonols decreased with decreasing [dye], the positive responses of these five dyes increased with decreasing [dye] (see Fig. 2, *bottom*, for a comparison of the negative responses of WW781 with the positive responses of RGA451). The near-optimal response of +20 %$\Delta F$ for RGA451 shown in Fig. 1 was obtained at 50 nM [dye], some 60 times lower than is necessary with WW781.

The far right column in Table 1 gives the equivalent alkyl chain lengths for the dyes (from Nyirgesy et al., 1988). For the 20 dyes surveyed, the correlation coefficient between the maximal response (%$\Delta F$) and the alkyl chain length was −0.26. If the three dyes which gave positive responses to $\Delta E_m$ are excluded, then the correlation coefficient becomes −0.45. Waggoner and co-workers reported a correlation coefficient of +0.64 between their response (fractional change in absorbance) measured in hemispherical bilayers, and the alkyl chain length.

Fig. 2 compares the initial fluorescence ($F$, top), change in fluorescence ($\Delta F$, *middle*), and response (%$\Delta F$, *bottom*) of RGA451 and WW781 at varied initial [dye]. As [dye] is decreased from 10 $\mu$M to 1 $\mu$M, the response of RGA451 increases from 0 to >30%, then plateaus between 1 and 0.1 $\mu$M [dye], and then slowly decreases. Note that $\Delta F$ for RGA451 has a maximum near 1 $\mu$M. The increase in response (%$\Delta F$) of RGA451 between 10 and 1 $\mu$M is therefore due to an increase in $\Delta F$ and a decrease in $F$.

## Absorption spectra in buffer and in cells

To determine whether dimerization or aggregation of dye occurs in cells or in buffer at the dye concentrations used in this study, absorption spectra of dye in buffer and in cell suspensions were determined at varied [dye]. The appearance of dimer peaks and/or of J bands with increasing [dye] would indicate aggregation (Herz, 1974). The spectra (Fig. 3) show no indication of any peaks in addition to the dye monomer peaks.

The absorption spectra of RGA451 did not show any significant changes upon hyperpolarization of cells with gramicidin (dashed line in Fig. 3 *d*). Cells treated with

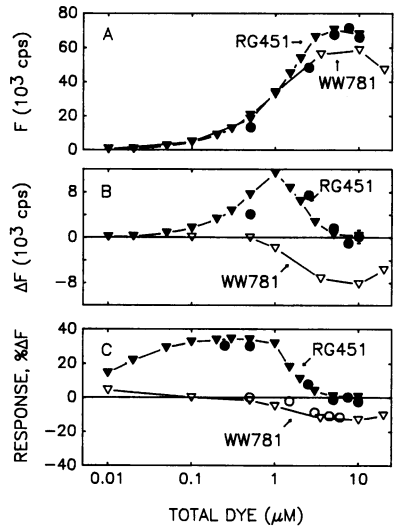


FIGURE 2 Comparison of $F$, $\Delta F$, and %$\Delta F$ for RGA451 (*solid symbols*) and WW781 (*open symbols*) at varied [dye]. These results are from two sets of experiments in which the membrane potential was changed with 317 ng gramicidin/ml of cell suspension. The inverted triangles represent the average of duplicate determinations in experiments where the initial [dye] was varied from 0.01–20 $\mu$M. The circles represent averages of two to four other experiments in which the binding of dye to cells was also measured, using 0.5–10 $\mu$M [dye]. $F$ and $\Delta F$ from the first set of experiments were scaled to the second set. Cells were suspended at 4% hematocrit in medium containing 1 mM KCl, 149 mM *N*-methyl-D-glucamine, and 5 mM Hepes, pH 7.4 at 25°C.

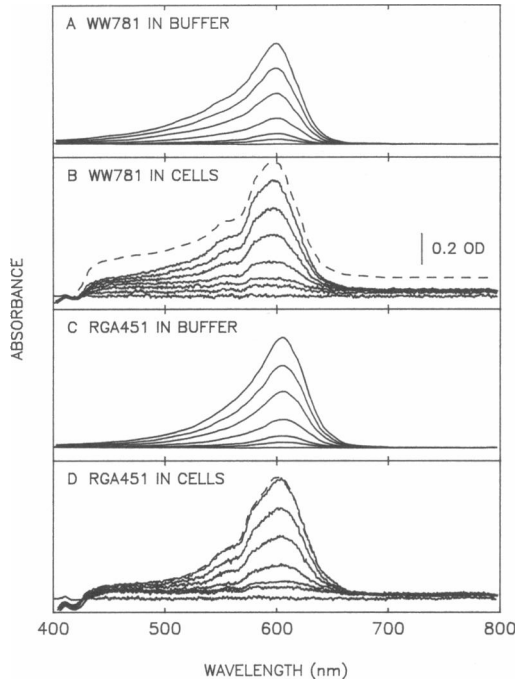


FIGURE 3 Absorption spectra of WW781 and RGA451 in buffer (*A*, *C*) and in cell suspensions (*B*, *D*). For cell suspensions, 60 μl of 50% HCT suspension was added to 7.5 ml of buffer containing 1 mM KCl, 149 mM *N*-methyl-D-glucamine, 5 mM Hepes, pH 7.4 at 25°C, and then 3 ml were transferred to the sample and reference cuvettes. After baseline adjustment, dye was added serially to the sample cuvette; an equal volume of ethanol was added to the reference. Absorbance was measured from 400 to 800 nm at a scan rate of 1 nm/s for dye in cell suspension and 2 nm/s for dye in buffer. At the end of each experiment with dye in cell suspension, spectra were measured after cells were hyperpolarized by the addition of gramicidin (final concentration, 20 μg/ml of cell suspension) to both sample and reference cuvettes (*dashed lines*).

WW781 show increased KCl efflux when hyperpolarized (see below, Fig. 8). The increased cell shrinkage due to the stimulated efflux would increase light scatter and therefore absorbance. The changes in the WW781 spectrum after hyperpolarization with gramicidin (*dashed line* Fig. 3 *b*) are consistent with increased shrinkage of cells.

## Interactions between oxonols and valinomycin

10 of the 20 oxonols were also tested for their responses to hyperpolarization of intact cells with valinomycin at 1 mM $[K]_o$ (Fig. 4 *B*, *open bars*), again using high $[K]_o$ (Fig. 4 *B*, *solid bars*) and leaky white ghosts (Fig. 4 *A*) as controls. In contrast to the results with gramicidin (Fig. 1), most of the oxonols, with the notable exception of WW781, gave large negative responses in intact red cells at 150 mM $[K]_o$ and in leaky white ghosts. These changes in fluorescence are attributable to interactions between the anionic dyes and the cationic K·valinomycin complex within the membrane.

Interaction between valinomycin and WW781 causes red-shifts and quenching of the uncorrected excitation and emission spectra of the dye (Fig. 5). For dye in buffer alone without ghosts (*top two panels*), and for dye in white ghost membranes (*bottom two panels*), fluorescence quenching by the K ionophore is more evident at 150 mM $[K]_o$ than at 0 mM $[K]_o$; quenching is also larger in buffer than in ghosts. At 0 mM $[K]_o$ (150 mM $[Na]_o$) with leaky ghosts, the effect is practically nil. The dependence on K of the extent of quenching, and its increase in buffer as compared with membranes, indicates that the anionic dye interacts with the cationic K·valinomycin complex rather than with neutral valinomycin.

## Properties of WW781 and RGA451

WW781 was chosen for further study because of its minimal interaction with valinomycin and also because of its use in previous studies of skeletal muscle (Vergara and Bezanilla, 1981; Baylor, 1983), heart (Dillon and Morad, 1981), and red blood cells (Freedman and Novak, 1983, 1984, 1989; Freedman and Miller, 1984; George et al., 1988*a*; Freedman et al., 1988). RGA451 was selected

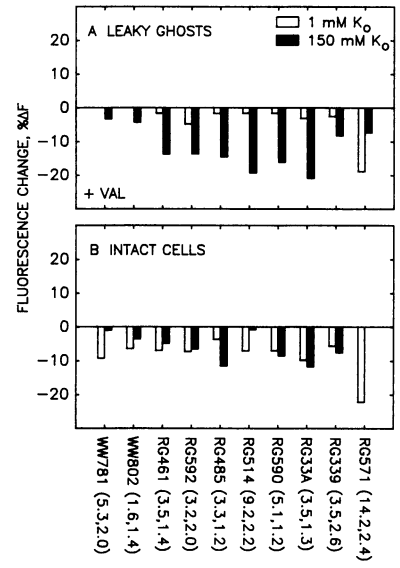


FIGURE 4 Responses of ten oxonols to 1 μM valinomycin in intact cells (*B*), with leaky ghosts as controls (*A*). The medium contained *x* mM KCl, (150 − *x*) mM NaCl, where *x* = 1 (*open bars*) or 150 (*solid bars*), and 5 mM Hepes, pH 7.4 at 25°C. Lack of bar indicates 0 %Δ*F*. The first number in parentheses indicates micromolar [dye], and the second number is percent hematocrit; for the conditions tested, these gave the maximal responses.

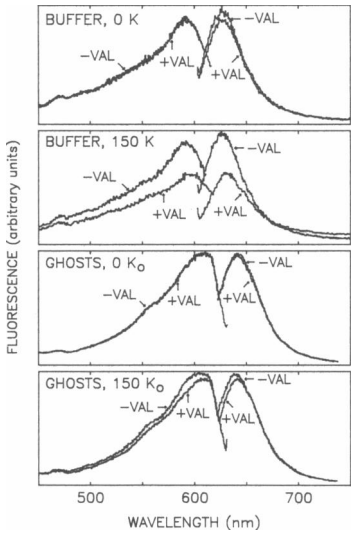


FIGURE 5 Spectral evidence for interactions between WW781 and K · valinomycin complex. Uncorrected excitation and emission spectra of WW781 before and after adding 1 μM valinomycin to dye in medium alone at 0 or 150 mM K (*top two panels*), or to leaky white ghosts (*bottom two panels*). The medium contained $x$ mM KCl, $(150 - x)$ mM NaCl, where $x = 0$ or 150, and 5 mM Hepes, pH 7.4 at 25°C. In each panel, the spectra are plotted as a percentage of the maximum fluorescence.

because of its large positive response (≥30%) with gramicidin (Figs. 1 and 2).

## Spectral responses to $\Delta E_m$

Fig. 6 shows uncorrected excitation and emission spectra for WW781 (*top*) and for RGA451 (*bottom*) in medium without cells (*lower traces* in each panel), and in 4% HCT suspensions before and after hyperpolarization with gramicidin (*upper traces* in each panel). Excitation of WW781 in medium alone is maximal at 600 nm, whereas the emission peak is at 645 nm. In a cell suspension, the excitation peak of WW781 is red shifted to 615 nm, whereas the emission peak is red shifted to 650 nm. The positions of these peaks for WW781 are consistent with those reported previously at lower HCT and [dye] with and without valinomycin (Freedman and Novak, 1983).

For RGA451, the excitation and emission spectra in medium alone have peaks at 590 and 643 nm, respectively. In cell suspensions, the excitation peak is red shifted to 615 nm, whereas the emission peak is red shifted to 652 nm. The slight dips at 540 and 575 nm in the excitation spectra of both dyes with cells are attributable to absorption by hemoglobin (Freedman and Novak, 1983).

No shift in the position of the excitation or emission peaks is evident for either dye after the addition of gramicidin (Fig. 6), or for WW781 with valinomycin (Freedman and Novak, 1983). Upon membrane hyperpolarization, the fluorescence intensity decreased for WW781 (negative response) and increased for RGA451 (positive response). Similar spectra (not shown) measured at 90 mM $[K]_o$ showed no changes after addition of gramicidin for either dye. The spectra for RGA451 at 1 mM $[K]_o$ also showed no changes at higher initial [dye]. In intact cells, RGA451 showed a valinomycin-induced response at 1 mM $[K]_o$, but not at 90 mM $[K]_o$ (data not shown); the results with valinomycin were comparable to those obtained with gramicidin (Fig. 6, *bottom*).

## Kinetic Responses

The half-time ($t_{1/2}$) of response of RGA451 to hyperpolarization with gramicidin is ~3.5 s (Fig. 7, *lower trace*); the $t_{1/2}$ is faster (by at least a factor of ~2) with valinomycin (Fig. 7, *middle trace*). Both responses are comparable to the mixing time ($t_{1/2} < 1$ s) for adding dye to dye in ethanol (Fig. 7, *upper trace*), and are therefore probably limited by the mixing time. For WW781, the valinomycin-induced response time is also comparable to the mixing time (Freedman and Novak, 1983; George et al., 1988*a*), whereas the response to gramicidin is some-

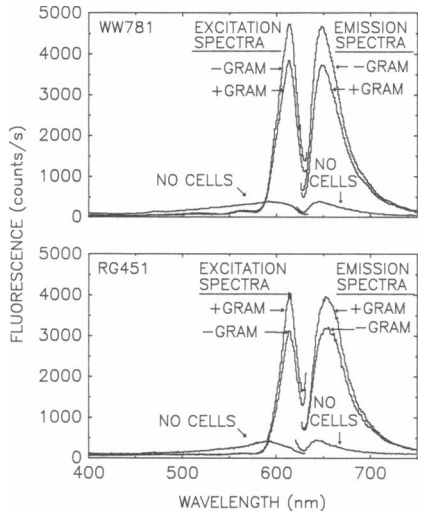


FIGURE 6 Potential-dependent excitation and emission spectra of WW781 (*top*) and RGA451 (*bottom*). The spectra of dye in 2.5 ml medium alone were first measured (*lower traces*). A 0.2-ml aliquot of dye solution was then replaced by an equal amount of 50% hematocrit cell suspension, and the spectra were remeasured (*upper traces*) before and after the addition of gramicidin (final concentration = 317 ng/ml suspension). External medium: 1 mM KCl, 149 mM *N*-methyl-D-glucamine, 5 mM Hepes, pH 7.4 at 25°C. Initial [dye]: WW781, 4.5 μM; RGA451, 0.5 μM. Excitation spectra were measured with the emission monochromator set at 642 nm for WW781 and 650 nm for RGA451. For emission spectra, the excitation monochromator was set at 615 nm for both WW781 and RGA451.

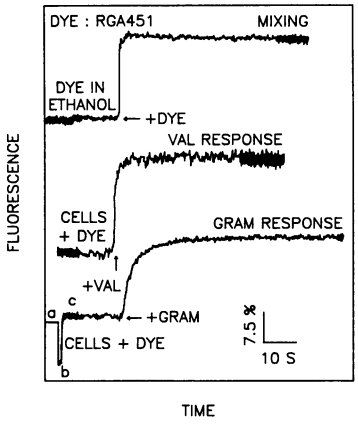


FIGURE 7 Response and mixing times of RGA451. The upper trace represents the change in fluorescence of dye in ethanol upon adding 2.4 $\mu$l of 1 mg/ml dye in ethanol. The middle trace represents the change in fluorescence of cells (4% hematocrit) with dye (1 $\mu$M) in buffer (1 mM KCl, 149 mM *N*-methyl-D-glucamine, 5 mM Hepes, pH 7.4 at 25°C) upon adding valinomycin. The bottom trace represents the change in fluorescence of cells with dye in medium upon adding gramicidin (317 ng/ml of suspension). The buffer and dye are the same in the bottom and middle traces. In both cases, the fluorescence is shown after subtraction of the baseline. Baseline subtraction is shown in the lower curve. Position *a* is the unsubtracted fluorescence, and *b* is the trace after subtraction. At position *c*, the pen speed is increased from 0.01 to 0.1 in/s.

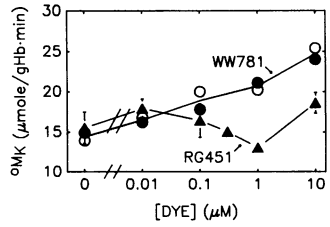


FIGURE 8 Effect of WW781 (*circles*) and RGA451 (*triangles*) on gramicidin-induced net K efflux ($^oM_K$). Open and filled circles are from two experiments with WW781, with the line drawn through the average. Filled triangles are the average fluxes in three experiments with RGA451. Error bars are standard deviations. The point at 0.3 $\mu$M dye represents a single experiment; at 1 $\mu$M, the error bar was smaller than the symbol. Cells were suspended at 4% hematocrit in medium containing 1 mM KCl, 149 mM *N*-methyl-D-glucamine, and 5 mM Hepes, pH 7.4 at 25°C.

what slower (not shown). Gramicidin is known to be a little slower than valinomycin in incorporating into planar lipid bilayers.

### Effects on gramicidin-induced net KCl efflux

Fig. 8 shows the gramicidin-induced net K efflux ($^oM_K$) in the presence of varied WW781 (*circles*) and of varied RGA451 (*filled triangles*). The stimulation of the gramicidin-induced KCl efflux by WW781 is similar to that noted in previous studies with valinomycin (Freedman et al., 1988). In contrast, gramicidin-induced net K efflux in the presence of RGA451 appears to decrease slightly between 0.1 and 1 $\mu$M initial [dye] and then to increase at higher [dye]. Net K efflux at 1 $\mu$M [RGA451] was 13.0 $\pm$ 0.3 $\mu$mol/g *Hb*/min, compared with 15.5 $\pm$ 2.0 (S.D., $n = 3$) without dye, a 16% decrease that was only marginally significant ($0.05 < P < 0.1$). The increase of K efflux above 1 $\mu$M [RGA451] is similar to that induced by WW781.

## Binding studies

Dye binding to cells was estimated in two different ways. In one approach, the dependence of dye fluorescence on hematocrit was analyzed on the basis of a single site model (see Appendix) by the procedure described in Methods. This model assumes that the bound dye forms a single homogeneous population, and is similar to analyses by others (e.g., Bashford and Smith, 1979; Fluhler et al., 1985). For the dyes WW781 and RGA451, the single-site model could fit the fluorescence data within experimental error (Fig. 9). For the 20 oxonols in Table 1, values for the apparent dissociation constant, $K_D$, ranged from 0.03 to 0.83 $\mu$M, whereas estimates for $n$ ranged from $0.5 \cdot 10^6$ to $4 \cdot 10^6$ sites/cell.

Because of the possibility that optical effects in turbid red cell suspensions might influence the recorded fluorescence intensity (Fig. 9), the binding of WW781 and of RGA451 to intact red cells was also measured directly. The fluorescence changes for WW781 during the protocol to assess binding directly (see Methods) are shown in Fig. 10. Note that the fluorescence of 3 $\mu$M WW781 in a red cell suspension is ~20 times that of dye in buffer, due to the greater quantum efficiency of dye in the membrane.

The fluorescence of supernatant dye, measured after centrifuging the cells (Fig. 10), is contaminated by the fluorescence of dye bound to hemoglobin which is present from hemolysis of ~0.1%. The binding and quantum efficiency of dye bound to hemoglobin were not determined, but this quantum efficiency is higher than that of dye in buffer. Consequently, dye absorbance was measured after centrifuging the suspensions, and was used instead of fluorescence to calculate the binding (see Methods). The extinction coefficients of WW781 (at 600 nm) and RGA451 (at 608 nm) showed no significant difference before and after addition of hemolysate corresponding to 0.5% hemolysis.

The fluorescence of WW781 in the cell suspension is stable for the duration of the measurement, ~3 min after addition of ionophore (Fig. 10). For WW781 in medium without cells, the rate of decline of fluorescence is only

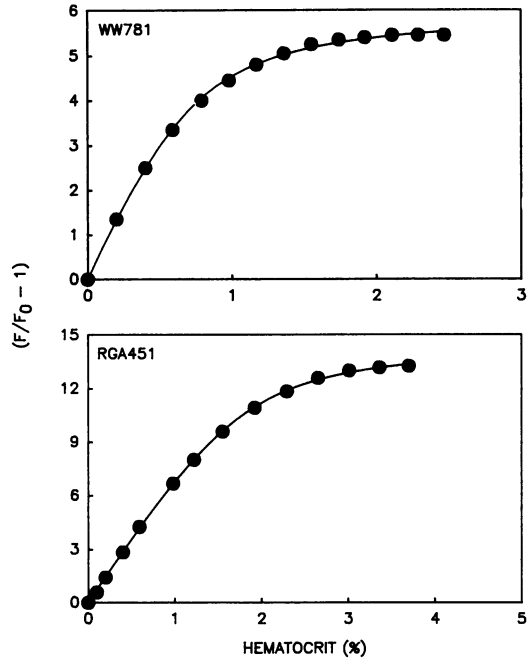


FIGURE 9 Fluorescence as a function of hematocrit for WW781 (*upper panel*) and RGA451 (*lower panel*). Fluorescence is expressed as $\epsilon - 1$, where $\epsilon = F/F_0$ (see Appendix). The solid lines represent the fit of the single site model (see Appendix) to the data. For WW781, a $K_d$ of 0.70 $\mu$M, an $n$ of 2.5 · $10^6$ sites/cell, and $\epsilon_b$ of 7 gave the best fit; for RGA451 a $K_d$ of 0.33 $\mu$M, an $n$ of 1.1 · $10^6$ sites/cell, and an $\epsilon_b$ of 15 gave the best fit.

$-0.1 \pm 0.1$ %$\Delta F$/min (S.D., $n = 6$), which is 10–20 times less than previously reported for the cyanines (Freedman and Novak, 1989). The absorbance of both dyes also was constant for 20 min, as was the fluorescence of either dye in red cell suspensions (not shown). Thus binding of dye to the cuvette is much less problematic with anionic oxonols than with the cationic cyanines.

Figs. 11 and 12 show the gramicidin-induced changes in the measured binding curves (bound dye vs. free dye) and apparent quantum efficiencies (AQE) of bound dye (F/[bound dye]) for WW781 and RGA451, respectively. In both figures, the upper two panels (*A* and *B*) are for 1 mM $[K]_o$, and the lower two panels are for 90 mM $[K]_o$ (*C* and *D*). The empty circles are before adding gramicidin and the filled circles are after ionophore.

For WW781 (Fig. 11), significant gramicidin-induced changes in binding were observed at 1 mM $[K]_o$ (Fig. 11 *A*), but not at 90 mM $[K]_o$ (Fig. 11 *C*). Although the apparent quantum efficiency of bound dye varies with [bound dye], the values with and without gramicidin (*open and solid circles*) fall approximately on the same curve (Fig. 11, *B* and *D*). At 90 mM $[K]_o$ (Fig. 11, *C* and *D*), no changes are observed in bound dye or apparent quantum efficiency upon adding gramicidin.

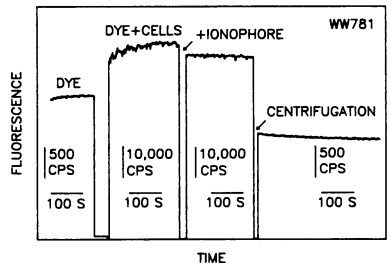


FIGURE 10 Fluorescence changes during protocol used in binding studies. First, fluorescence and absorbance of dye (3 $\mu$M WW781 in this case) in medium alone is measured. Then, 0.2 ml of dye solution in medium is replaced with a 50% hematocrit cell suspension (final hematocrit = 4%), and the fluorescence is recorded before and after the addition of ionophore (valinomycin). Finally, the cell suspension is centrifuged, and the absorbance of the supernatant is measured at 615 nm. Binding was calculated from the difference between the initial dye, and the free dye remaining after centrifugation (see Materials and Methods for details).

For RGA451 (Fig. 12), significant gramicidin-induced changes in dye binding are also observed at 1 mM $[K]_o$ (Fig. 12 *A*), but not at 90 mM $[K]_o$ (Fig. 12 *C*). However, these changes in dye binding do not correlate with the gramicidin-induced positive fluorescence changes (Figs. 1, 2 *C*, 6, and 7). The apparent quantum efficiency of bound dye is approximately the same with and without gramicidin at 90 mM $[K]_o$ (Fig. 12 *D*), but unlike WW781 falls on different curves at 1 mM $[K]_o$

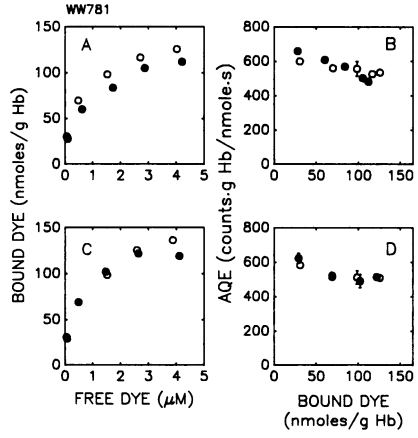


FIGURE 11 (*A*) Binding curve for WW781 at 1 mM $[K]_o \pm$ gramicidin (*filled and open circles*, respectively) (see Fig. 8 and Materials and Methods for details). (*B*) Apparent quantum efficiency of bound dye ($F_{bound}$/$[Dye]_{bound}$) for the experiment in (*A*). (*C*, *D*) Binding curve and apparent quantum efficiency of WW781 at 90 mM $[K]_o$. Error bars represent standard error of the mean of three repetitions. Cells suspended at 4% hematocrit in medium containing: $x$ mM KCl ($x$ = 1 or 90), (150 − $x$) mM *N*-methyl-D-glucamine, and 5 mM Hepes, pH 7.4 at 25°C.

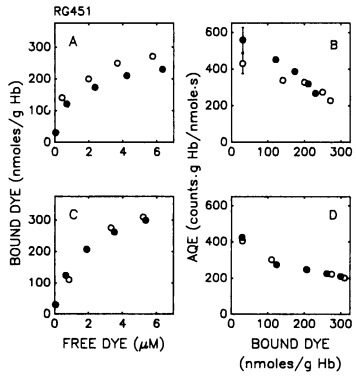


FIGURE 12 (*A, B*) Binding curve and apparent quantum efficiency for RGA451 at 1 mM $[K]_o$ ± gramicidin (*solid and open circles*, respectively). (*C, D*) Binding curve and apparent quantum efficiency of RGA451 at 90 mM $[K]_o$. Error bars represent standard error of the mean of three repetitions. Cells suspended at 4% hematocrit in medium containing $x$ mM KCl ($x = 1$ or 90), $(150 - x)$ mM *N*-methyl-D-glucamine, 5 mM Hepes, pH 7.4 at 25°C.

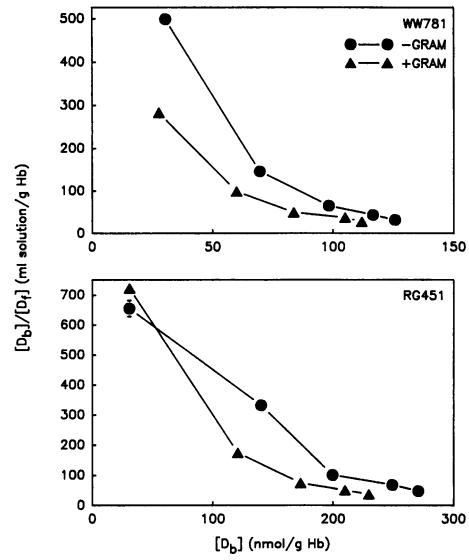


FIGURE 13 Scatchard plots of dye binding. The binding data shown in Figs. 11 *A* and 12 *A* for WW781 and RGA451 before (*solid circles*) and after (*solid triangles*) addition of gramicidin were replotted with the ratio of bound to free dye on the ordinate and with bound dye on the abscissa.

(Fig. 12 *B*). At 0.5 μM $[dye]_{initial}$ and 4% hematocrit, ~90% of the total dye is membrane associated.

A comparison of binding curves (before adding gramicidin) for WW781 and RGA451 (Figs. 11 and 12, *open circles*) indicates that the concentration of free dye required for half-maximal binding is ~0.5 μM for both dyes, whereas the maximal binding of RGA451 is approximately twice that of WW781. If the dyes are assumed to function by a single site model (see Appendix), these concentrations would be the dissociation constants ($K_d$) for the dyes. A free dye concentration of 0.5 μM corresponds to a total dye concentration (before addition of cells) of 1.4 μM for WW781 and 2.4 μM for RGA451. Curiously, RGA451 responds optimally below its $K_d$, whereas WW781 exhibits optimal responses above its $K_d$ (see Fig. 2).

The direct measurements of dye binding were also expressed in terms of Scatchard plots of $[dye]_{bound}/[dye]_{free}$ vs. $[dye]_{bound}$ (Fig. 13). For both WW781 and RGA451, these curves could be expressed by the sum of at least two straight lines, indicating the presence of at least two types of binding sites in the membrane—a high and a low affinity site. Thus, despite the excellent fit of the fluorescence data by the single-site model (Fig. 9, Table 1), the curvature of the Scatchard plots (Fig. 13) forces rejection of the single-site model.

The Scatchard plots indicate ~$2.6 \cdot 10^6$ low-affinity sites/cell for WW781 and $5.8 \cdot 10^6$ low-affinity sites/cell for RGA451, with little dependence of the number of low-affinity sites on membrane potential for both dyes (Fig. 13). Upon hyperpolarization with gramicidin, the dissociation constant of the low-affinity site increased from ~5 to 8 μM for WW781 and from ~6 to 9 μM for RGA451. For WW781, the number of high affinity binding sites was $<1.4 \cdot 10^6$ sites/cell with a $K_d$ <0.16 μM, and the affinity of these sites also decreased upon hyperpolarization, consistent with an on–off mechanism. More data would be needed to quantitate further any possible change in the number of high affinity sites for WW781 with hyperpolarization. For RGA451, the number of high affinity sites with $K_D$ of ~0.33 μM decreased from ~$4.0 \cdot 10^6$ sites/cell to $<2.6 \cdot 10^6$ sites/cell upon hyperpolarization, and their affinity increased. The combination of these two effects with RGA451 can result in a decrease of dye binding.

## DISCUSSION

### Dye survey

20 oxonols were surveyed for their ability to report changes in red blood cell membrane potential induced with gramicidin or valinomycin at 1 mM $[K]_o$ (Table 1 and Fig. 1). The oxonols, which are a subset of those studied by Waggoner and co-workers in hemispherical bilayers (George et al., 1988*a*, *b*; Nyirgesy et al., 1988) are presumed to be membrane impermeant because of their fast responses and a fixed negative anchor charge. The survey by Waggoner and co-workers indicated that these dyes function by an "on–off" mechanism.

The response of these oxonols in red cells differs from that in the artificial membranes in two ways: whereas

Waggoner and co-workers found a positive correlation between response and the alkyl chain length, a negative correlation was found with red blood cells. Also, five of the 20 dyes surveyed in red blood cells exhibited positive responses over some range of dye concentration, implying the existence of a new mechanism for the potentiometric response of these oxonols.

Comparison of the two dye surveys is difficult because the methods used by Waggoner and co-workers differed from this study in the following ways: (*a*) They used an artificial membrane system in which the inner and outer leaflets of the bilayer are identical; in contrast, the red-cell membrane is asymmetric, the inner leaflet being more polar than the outer leaflet. (*b*) The membrane was saturated with dye at the concentrations they used (6 $\mu$M; Nyirgesy et al., 1988) whereas dye concentrations used in this work spanned ranges where the membrane was saturated and unsaturated. Positive responses are seen at concentrations where the membrane is probably far from saturation. (*c*) They measured absorbance changes, whereas fluorescence changes were measured in this work. These two quantities are proportional only at low [dye]. (*d*) Their absorbance changes were measured with 5-ms pulse trains of potential. The system is therefore not at equilibrium, and these pulse trains may result in depletion of dye in the unstirred layer adjacent to the membrane. Experiments reported in this paper were done under equilibrium conditions: measurements were taken only when the fluorescence had stabilized to a new value. Dye concentration in the unstirred layer was probably the same as in the bulk solution.

In addition, the responses of five of the dyes surveyed in this work are inconsistent with an "on–off" mechanism. When cells are added to a solution of dye in buffer, the intensity of fluorescence increases by a factor of 10–20 (Figs. 6, 10). This increase is attributable to incorporation of dye into the cell membrane where the fluorescence quantum efficiency is higher because of the lower polarity of the environment. If these anionic dyes report $\Delta E_m$ by an "on–off" mechanism, hyperpolarization is expected to drive dye off the membrane, thus reducing the total fluorescence of the cell suspension (negative $\Delta F/F$). The positive responses for five of the dyes surveyed, RGA451, RGA459, RGA497, RGA500, and RGA561, indicate a different mechanism of action for these dyes. These dyes exhibit positive responses at 0.5–2 $\mu$M [dye]; at higher [dye], their response is either zero or negative.

10 of the dyes were examined for their response to $\Delta E_m$ induced by valinomycin (Fig. 4). With this ionophore, most dyes showed large artifactual responses in intact cells at 150 mM $[K]_o$ and also in leaky ghosts, suggesting interactions between anionic dyes and the cationic K·valinomycin complex. Of the ten dyes surveyed, only WW781 showed a minimal artifactual response in intact red cells (Fig. 4). However, in buffer alone without cells or in ghost membranes, excitation and emission spectra of WW781 were red shifted and quenched (Fig. 5), indicating that WW781 also interacts with the K·valinomycin complex.

The dye structures in Table 1 indicate that four of the five dyes which show positive responses have bulky groups in the $R_2$ position (a phenyl for RGA451, a t-butyl for RGA500, and a $CO_2$-ethyl for RGA567). However, generalizations cannot be made, because RGA459, which also exhibits significant positive response, has a structure similar to WW781 or RGA571. The pK's of the phenolic hydroxyl groups of the various analogues are unknown.

The excitation and emission spectra for WW781 before and after adding gramicidin (Fig. 6, *top*) are similar to those reported previously (Freedman and Novak, 1983) at lower HCT and [dye] before and after adding valinomycin. The spectra for RGA451 at low [dye] (Fig. 6, *bottom*) reflect its positive fluorescence response. No detectable wavelength shift could be seen upon hyperpolarization; a spectral shift might indicate movement of dye within the membrane between sites of varying polarity. Although spectral shifts were not detected, they cannot be ruled out because the amount of dye involved may be too small.

## Binding studies

As previously concluded for artificial membranes (George et al., 1988*a*), both WW781 and RGA451 show significant changes in binding upon membrane hyperpolarization at $[K]_o$ = 1 mM (Figs. 11 *A* and 12 *A*). No such binding changes were observed at 90 mM $[K]_o$ (Figs. 11 *C* and 12 *C*).

The observed change in WW781 binding of 10 ± 2% (Fig. 11 *A*) in binding corresponds to a fluorescence change of 13.3 ± 0.2% (Fig. 2 *C*). These values are consistent with the hypothesis that the fluorescence change is due to changes in dye binding to the membrane. Unlike WW781, no correlation was observed between changes in membrane binding of RGA451 and its fluorescence response. At 1 $\mu$M [dye] where the response was large, there was no detectable change in $[dye]_{bound}$ (Fig. 12 *A*). At higher [dye], where significant changes in membrane-bound dye were observed, no changes in fluorescence were seen (see Figs. 2 *C* and 12 *A*).

The variation of the apparent quantum efficiency (AQE) of bound WW781 with $[dye]_{bound}$ (Fig. 11 *B* and *D*) also supports the hypothesis that the response of this dye is mediated by an on–off mechanism. Because fluorescence ($F$) is a nonlinear function of [dye], the apparent quantum efficiency (defined as $F$/[dye]) depends on [dye] as follows: at very low [dye], $F$ is approximately

linear with [dye], and the apparent quantum efficiency is constant, with the true quantum efficiency being the limiting value at zero [dye]; at high [dye], the fluorescence saturates, and the apparent quantum efficiency therefore varies inversely with [dye]. This curve of AQE vs. [dye] is specific for a dye with a particular quantum efficiency. With a different quantum efficiency, this curve would have a different slope. However, if only the concentration of dye is changed, then its AQE should fall on this same curve.

If the dye responds by an on–off mechanism, then the amount of bound anionic dye should decrease with membrane hyperpolarization. Because addition of ionophore would decrease $[dye]_{bound}$, AQE before and after the addition of ionophore would fall on the same curve (see Figs. 11 *B* and *D*). However, if the concentration of bound dye remains the same upon hyperpolarization, but the quantum efficiency changes, then AQE of bound dye before and after ionophore should fall on different curves.

The apparent quantum efficiency of bound WW781 before and after addition of gramicidin falls approximately on the same curve (Fig. 11 *B*)—an observation consistent with an on–off mechanism. For RGA451, the apparent quantum efficiency of bound dye at low total dye appears to fall on different curves before and after the addition of gramicidin (Fig. 12 *B*). This change in AQE indicates that the fluorescence of membrane-bound RGA451 is potential dependent.

The Scatchard plots (Fig. 13) of the direct measurements of binding revealed the presence of at least two populations of sites in the membrane, a feature that would have been missed by simply fitting fluorescence as a function of hematocrit (Table 1, Fig. 9). For both dyes, the dissociation constant of the low affinity sites appeared to increase upon hyperpolarization. For WW781, the affinity of the high-affinity sites appeared to decrease with hyperpolarization. For RGA451, the affinity of the high-affinity sites increased whereas the number of sites decreased upon hyperpolarization.

## A two-site binding model

Both WW781 and RGA451 exhibit apparent solvatochromic red shifts in their excitation spectra upon addition of dye to red cells (Fig. 6). However, no solvatochromic or electrochromic shift was detectable in the absorbtion spectra of either dye (Fig. 3). Although an electrochromic mechanism could conceivably give rise to a fluorescence change in the range of 10–30% (Waggoner and Grinvald, 1977), the binding studies (Figs. 11–13) suggest an on–off mechanism for WW781 and a potential-dependent movement within the membrane between two sites of different polarity for RGA451.

A possible model to explain the two types of potentiometric responses of oxonols is shown schematically in Fig. 14. This model is based on the following assumptions: (*a*) dye in the membrane is distributed between two sites (I and II); (*b*) dye can only move between I and II and between II and the aqueous medium; (*c*) for dyes with a positive response, dye in site I has a lower quantum efficiency than in II, whereas for dyes with a negative response either the quantum efficiencies are comparable in sites I and II but higher than in the aqueous buffer, or, alternatively, the dye does not have access to site I.

For permeant oxonols, the membrane-water partition coefficient is of the order of $10^4$ (Apell and Bersch, 1987). The greater solubility of analogues of RGA451 and WW781 in butanol as compared with buffer also supports a large membrane-water partition coefficient for impermeant oxonols (George et al., 1988*a*). The membrane-water partition coefficient of impermeant oxonols can therefore be reasonably assumed to be high.

At low [dye] (Fig. 14 *A*), because of the high membrane-water partition coefficient, most of the cell-associated dye will be membrane-bound, either in site I or II, and a large number of both type of sites will be empty. Upon hyperpolarization dye moves from I to II, but because of the large membrane-water partition coefficient of the dye, very little moves from II into the medium. Such a movement of RGA451 would result in a positive response if the quantum efficiency of dye in site II is greater than in I. A similar movement of WW781 would result in a negligible response at low [dye] if the quantum efficiencies for this dye in sites I and II are comparable, or if the amount of dye driven from site II is small.

At high [dye] (Fig. 14 *B*), most of the membrane sites of both types will be occupied. Because hyperpolarization at these dye concentrations will result in movement of dye from I to II only if some dye also moves from II into the buffer, there will be a net movement of dye from I into the

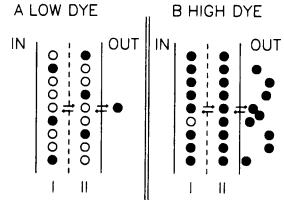


FIGURE 14 Schematic representation of proposed two-site model for mechanism of potentiometric oxonols in red blood cells at low (*A*) and high (*B*) initial [dye]. Solid circles represent dye molecules. Open circles are empty membrane binding sites. Single solid lines are membrane boundaries. Dashed lines represent boundary between sites I and II in the membrane. IN and OUT are the cell interior and exterior, respectively. Arrows represent possible paths taken by the dye.

aqueous buffer. The magnitude and sign of the fluorescence change upon hyperpolarization at high [dye] now depends on the relative quantum efficiencies of dye in I and in buffer. According to the model, the negligible response at high [RGA451] could result from these quantum efficiencies being approximately equal. The model could explain the negative responses of RGA459 and RGA497 at high [dye] if the quantum efficiency of these dyes in I is significantly higher than in buffer. These dyes are presumed to have access to site I because they give positive responses at low [dye]. The negative response at high [WW781], which gives no positive response at low [dye], could result either from a movement from I to buffer (if its quantum efficiencies in I and II are comparable), or from II to buffer if this dye does not reach site I.

It should be noted that Fig. 14 indicates that the two sites are located in the inner and outer leaflets of the membrane, a representation made purely for convenience and without supportive evidence. Moreover, it is difficult to understand how dye could reach the inner hemileaflet and still be impermeant.

The high membrane-water partition coefficient also precludes the hypothesis that site I is within the cell (i.e., dye permeates into the cell in spite of the anchor charge). Analysis of the binding curves (Figs. 11 *A* and 12 *A*) establishes that ~90% of the total dye is bound at 0.5 $\mu$M total [dye], corresponding to 0.06 $\mu$M free dye. This finding, and the proportionality between suspension fluorescence and [dye] at low [dye] (Fig. 2 *A*), together imply that an increase in the suspension fluorescence by 30% must be accompanied by an increase in $[dye]_{bound}$ by a similar amount. Because 90% of the dye is already bound to the membrane at the low dye concentrations where positive fluorescence changes are seen, it seems unlikely that the positive response of RGA451 is due to increases in $[dye]_{bound}$ from dye inside the cell.

## Interactions between dye and membrane

Theoretically, the membrane potential is given by the Goldman equation:

$$E_m = (RT/F) \ln [(P_K K_i + P_{Cl} Cl_o)/(P_K K_o + P_{Cl} Cl_i)] \quad (4)$$

where P's are the permeabilities of the different ions, and $K_i$, $Cl_i$, and $K_o$, $Cl_o$ represent ion concentrations inside and outside the cell. In the presence of the K ionophore valinomycin, or with gramicidin in choline medium, $E_m$ shifts from the Cl equilibrium potential of $-9$ mV toward the K equilibrium potential of $-122$ mV (at 1 mM $[K]_o$). Because WW781 stimulates the chloride conductance (increases $P_{Cl}$), the magnitude of $\Delta E_m$ with ionophore would be less than in the absence of dye. Thus WW781 will underestimate $\Delta E_m$. Data in this paper (Fig. 8) indicate that at their respective optimal concentrations, the stimulation of net Cl fluxes is much less with RGA451 than with WW781.

## CONCLUSIONS

The main conclusion from the results in this paper is that most impermeant oxonols report $\Delta E_m$ in red blood cells by an on–off mechanism, as concluded by George et al. (1988*a*). However, some of these dyes report $\Delta E_m$ in red cells by a different mechanism. These results reaffirm our previous conclusion that the mechanism of dye action depends on the specific system and dye (Waggoner and Grinvald, 1977; Freedman and Hoffman, 1979*b*).

Because large positive responses are observed at <1 $\mu$M [dye], with minimal effect on chloride conductance, RGA451 may be more suitable than WW781 as a rapidly responding optical potentiometric indicator in red blood cells. However, further studies would be needed to test its utility more completely.

Waggoner and Grinvald (1977) suggested that the two most likely mechanisms of response of impermeant dyes are dye translocation between the membrane and the surrounding medium (on–off), or between two sites within the membrane, with the dye in each site sensing different local conditions. The two-site model proposed in this paper suggests that at least some impermeant oxonols work by a combination of these two mechanisms.

What are the two sites within the membrane? The inner and outer leaflets of the red-cell plasma membrane have different polarity (Rothman and Lenard, 1977; Williamson et al., 1985). Because dye fluorescence depends on solvent polarity, a translocation of dye between these hemileaflets may result in a change in fluorescence. This membrane asymmetry of the red blood cell could explain why positive responses were observed in red blood cells, but not in symmetric artificial membranes. Whether or not oxonols actually reach the inner polar hemileaflet is unknown. Despite the lack of knowledge of the actual location of the dyes, the two-site model proposed here is quite capable of explaining the qualitative features of the response of all impermeant oxonols so far examined.

## APPENDIX

### Analysis of dye-membrane association

The association of dye with membrane was examined according to a model in which dye is assumed to associate with sites on the membrane

(Bashford and Smith, 1979):

$$D + M \rightleftharpoons B, \quad \text{(A1)}$$

where $D$ is the dye, $M$ is the association site, and $B$ is the dye-membrane complex. The dissociation constant $K_d$ ($\mu$mol/l suspension) is defined as

$$K_d = (d - b)(mn - b)/b, \quad \text{(A2)}$$

where $d$ is the total dye concentration in the suspension ($\mu$mol/l suspension), $b$ is the concentration of the dye-membrane complex ($\mu$mol/l suspension), $m$ is the concentration of cells (ml cells/l suspension), and $n$ is the concentration of association sites ($\mu$mol/ml cells). Eq. A2 is quadratic in $b$, and can be solved for the membrane-associated dye $b$:

$$b = 0.5 \cdot (K_d + d + nm) - \sqrt{[(K_d + d + nm)^2 - 4\,dnm]}. \quad \text{(A3)}$$

(Only the negative root of Eq. A2 is considered, to satisfy the condition that $b = 0$ when $d$ is 0).

The enhancement parameter $\epsilon$ was defined as (Bashford and Smith, 1979)

$$\epsilon = F/F_0, \quad \text{(A4)}$$

where $F_0$ is the fluorescence of the suspension at zero hematocrit, and $F$ is the fluorescence with membrane. If $c$ is the fraction of membrane-associated dye ($c = b/d$), then the enhancement parameter is related to $c$ by

$$c = b/d = (\epsilon - 1)/(\epsilon_b - 1), \quad \text{(A5)}$$

where $\epsilon_b$ is the enhancement if all the dye were membrane-associated. Substituting Eq. A3 into Eq. A5 gives $\epsilon$ as a function of hematocrit ($m$):

$$\epsilon = 1 + (\epsilon_b - 1) \cdot \{(K_d + d + nm) - \sqrt{[(K_d + d + nm)^2 - 4dnm]}\}/2d. \quad \text{(A6)}$$

From the fluorescence of dye at different hematocrits, the enhancement parameter $\epsilon$ was calculated with Eq. A4. The calculated $\epsilon$ was then fit by Eq. A6 with a nonlinear least-square algorithm (Hamilton, 1964). This fit provided estimates of the apparent $K_d$, $n$, and $\epsilon_b$. The units for $n$ were converted to sites/cell assuming that 1 $\mu$mol/ml cells is equivalent to $5 \cdot (10)^7$ sites/cell.

We thank Dr. Alan S. Waggoner for providing the oxonol dyes. We also thank Dr. L. B. Cohen for comments on the manuscript.

This research was supported by NIH grant GM28839 to Dr. Freedman. Dr. Pratap was a Fellow of the American Heart Association, New York State Affiliate.

*Received for publication 22 August 1988 and in final form 23 October 1989*

## REFERENCES

Apell, H.-J., and B. Bersch. 1987. Oxonol VI as an optical indicator for membrane potentials in lipid vesicles. *Biochim. Biophys. Acta.* 903:480–494.

Bashford, C. L., and J. C. Smith. 1979. The determination of oxonol-membrane binding parameters by spectroscopic methods. *Biophys. J.* 25:81–85.

Bashford, C. L., B. Chance, J. C. Smith, and T. Yoshida. 1979. The behavior of oxonol dyes in phospholipid dispersions. *Biophys. J.* 25:63–85.

Baylor, S. M. 1983. Optical studies of excitation-contraction coupling using voltage-sensitive and calcium-sensitive probes. *In* Handbook of Physiology. L. D. Peachey and R. H. Adrian, editors. American Physiology Society, Bethesda, MD. 355–379.

Bifano, E. M., T. S. Novak, and J. C. Freedman. 1984. Relationship between the shape and the membrane potential of human red blood cells. *J. Membr. Biol.* 82:1–13.

Cabrini, G., and A. S. Verkman. 1986*a*. Mechanism of interaction of the cyanine dye diS-$C_3$(5) with renal brush-border vesicles. *J. Membr. Biol.* 90:163–175.

Cabrini, G., and A. S. Verkman. 1986*b*. Potential-sensitive response mechanism of diS-$C_3$(5) in biological membranes. *J. Membr. Biol.* 92:171–182.

Dillon, S., and M. Morad. 1981. A new laser scanning system for measuring action potential propagation in the heart. *Science* (*Wash. DC*). 214:453–456.

Dodge, J. T., C. Mitchell, and D. J. Hanahan. 1963. The preparation and chemical characteristics of hemoglobin-free ghosts of human erythrocytes. *Arch. Biochem. Biophys.* 100:119–130.

Dragsten, P. R., and W. W. Webb. 1978. Mechanism of the membrane potential sensitivity of the fluorescent probe merocyanine 540. *Biochemistry.* 17:5228–5240.

Fluhler, E., V. G. Burnham, and L. M. Loew. 1985. Spectra, membrane binding, and potentiometric responses of new charge shift probes. *Biochemistry.* 24:5749–5755.

Freedman, J. C., and J. F. Hoffman. 1979*a*. Ionic and osmotic equilibria of human red blood cells treated with nystatin. *J. Gen. Physiol.* 74:157–185.

Freedman, J. C., and J. F. Hoffman. 1979*b*. The relation between dicarbocyanine dye fluorescence and the membrane potential of human red blood cells set at varying Donnan equilibria. *J. Gen. Physiol.* 74:187–212.

Freedman, J. C., and P. C. Laris. 1981. Electrophysiology of cells and organelles: studies with optical potentiometric indicators. *Int. Rev. Cytol.* 12:(Suppl.)177–246.

Freedman, J. C., and P. C. Laris. 1988. Optical potentiometric indicators for nonexcitable cells. *In* Spectroscopic Membrane Probes. L. Loew, editor. CRC Press, Boca Raton, FL. 3:1–49.

Freedman, J. C., and T. S. Novak. 1983. Voltages associated with Ca-induced K conductance in human red blood cells. Studies with a fluorescent oxonol dye, WW781. *J. Membr. Biol.* 72:59–74.

Freedman, J. C., and C. Miller. 1984. Membrane vesicles from human red blood cells in planar lipid bilayers. *Ann. NY Acad. Sci.* 435:541–544.

Freedman, J. C., and T. S. Novak. 1984. $Cl^-$ conductance of valinomycin-treated human red blood cells. *J. Gen. Physiol.* 84:18*a*. (*Abstr.*)

Freedman, J. C., and T. S. Novak. 1989. Optical measurement of membrane potential in cells, organelles and vesicles. *Methods Enzymol.* 172:102–122.

Freedman, J. C., E. M. Bifano, L. M. Crespo, P. R. Pratap, R. Walenga, R. E. Bailey, S. Zuk, and T. S. Novak. 1988. Membrane potential and the cytotoxic Ca cascade of human red blood cells. *In* Cell Physiology of Blood. R. B. Gunn and J. C. Parker, editors. *Soc. Gen. Physiol. Ser.*, Rockefeller Univ. Press, New York. 217–231.

George, E. B., P. Nyirjesy, M. Basson, L. E. Ernst, P. R. Pratap, J. C.

Freedman, and A. S. Waggoner. 1988*a*. Impermeant potential-sensitive oxonol dyes. I. Evidence for an "on–off" mechanism. *J. Membr. Biol.* 103:245–253.

George, E. B., P. Nyirjesy, P. R. Pratap, J. C. Freedman, and A. S. Waggoner. 1988*b*. Impermeant potential-sensitive oxonol dyes. III. The dependence of the absorption signal on membrane potential. *J. Membr. Biol.* 105:55–64.

Guillet, E. G., and G. A. Kimmich. 1981. DiO-$C_3(5)$ and diS-$C_3(5)$: interactions with RBC, ghosts and phospholipid vesicles. *J. Membr. Biol.* 59:1–11.

Gupta, R. K., B. M. Salzberg, A. Grinvald, L. B. Cohen, K. Kamino, S. Lesher, M. B. Boyle, A. S. Waggoner, and C. H. Wang. 1981. Improvements in optical methods for measuring rapid changes in membrane potential. *J. Membr. Biol.* 58:123–137.

Hamilton, W. C. 1964. Statistics in Physical Science. The Ronald Press Company. 150–157.

Herz, A. H. 1974. Dye–dye interactions of cyanines in solution at AgBr surfaces. *Photogr. Sci. Eng.* 18:323–335.

Hladky, S. B., and T. J. Rink. 1976. Potential difference and the distribution of ions across the human red blood cell membrane: a study of the mechanism by which the fluorescent cation, diS-$C_3(5)$ reports membrane potential. *J. Physiol. (Lond.).* 263:287–319.

Hoffman, J. F., and P. C. Laris. 1974. Determination of membrane potential in human and amphiuma red blood cells by means of a fluorescent probe. *J. Physiol. (Lond.).* 239:519–552.

Loew, L. M., and L. L. Simpson. 1981. Charge-shift probes of membrane potential. A probable electrochromic mechanism for *p*-aminostyrylpyridinium probes on a hemispherical lipid bilayer. *Biophys. J.* 34:353–365.

Loew, L. M., L. B. Cohen, B. M. Salzberg, A. L. Obaid, and F. Bezanilla. 1985. Charge-shift probes of membrane potential. Characterization of aminostyrylpyridinium dyes on the squid giant axon. *Biophys. J.* 47:71–77.

London, J. A., D. Zecevic, and L. B. Cohen. 1988. Simultaneous monitoring of many individual neurons in molluscan ganglia using a multielement detecting system. *In* Spectroscopic Membrane Probes. L. Loew, editor. CRC Press, Boca Raton, FL. 3:101–114.

Nyirjesy, P., E. B. George, R. K. Gupta, M. Bassom, P. R. Pratap, J. C. Freedman, and A. S. Waggoner. 1988. Impermeant potential-sensitive oxonol dyes. II. The dependence of the absorption on the length of alkyl substituents attached to the dye. *J. Membr. Biol.* 105:45–53.

Ross, W. N., B. M. Salzberg, L. B. Cohen, and H. V. Davila. 1974. A large change in dye absorption during the action potential. *Biophys. J.* 14:983–986.

Rothman, R. E., and J. Lenard. 1977. Membrane asymmetry. *Science (Wash. DC.).* 195:743–753.

Sims, P. J., A. S. Waggoner, C.-H. Wang, and J. F. Hoffman. 1974. Studies on the mechanism by which cyanine dyes measure membrane potential in red blood cells and phosphatidylcholine vesicles. *Biochemistry.* 13:3315–3330.

Tsien, R. Y., and S. B. Hladky. 1978. A quantitative resolution of the spectra of a membrane potential indicator, diS-$C_3(5)$, bound to cell components and to red blood cells. *J. Membr. Biol.* 38:73–97.

Vergara, J., and Bezanilla, F. 1981. Optical studies of E-C coupling with potentiometric dyes. *In* The Regulation of Muscle Contraction: Excitation-Contraction Coupling. A. D. Grinnell and M. A. B. Brazier, editors. Academic Press, New York. 67–77.

Waggoner, A. S. 1979. Dye indicators of membrane potential. *Annu. Rev. Biophys. Bioeng.* 8:47–68.

Waggoner, A. S., and A. Grinvald. 1977. Mechanism of rapid optical changes of potential sensitive dyes. *Ann. NY Acad. Sci.* 303:217–241.

Waggoner, A. S., C. H. Wang, and R. L. Tolles. 1977. Mechanism of potential-dependent light absorption changes of lipid bilayer membranes in the presence of cyanine and oxonol dyes. *J. Membr. Biol.* 33:109–140.

Williamson, P., L. Algarin, J. Bateman, H.-R. Choe, and R. A. Schlegel. 1985. Phospholipid asymmetry in human erythrocyte ghosts. *J. Cell Physiol.* 123:209–214.

Wolf, B. E., and A. S. Waggoner. 1986. Optical studies of the mechanism of membrane potential sensitivity of merocyanine 540. *Soc. Gen. Physiol. Ser.* 40:101–113.